

# Theoretical Study of the Deprotonation of Nitriles, $\text{RCH}_2\text{CN}$ : Ab Initio and PM3 Calculations of Intermediate Aggregates and Transition States

Rainer Koch, Bernd Wiedel, and Ernst Anders\*

*Institut für Organische Chemie und Makromolekulare Chemie der Universität Jena,  
Humboldtstrasse 10, D-07743 Jena, Germany*

Received November 1, 1995\*

The intermediates and transition state for the deprotonation of acetonitrile, **7**, with dimeric lithiumamide  $[\text{LiNH}_2]_2$ , **8**, which leads to the dianion complex  $[\text{CH}_2\text{CN}/\text{NH}_2]^{2-} \cdot 2 \text{Li}^+$ , **14**, have been calculated by ab initio (MP2(full)/6-31+G\*/MP2(full)/6-31+G\*), DFT (Becke3LYP/6-311+G\*, DGAUSS DZP/A1), and semiempirical methods. This reaction is initiated by the formation of a 4-ring-dimer/nitrile complex, **9**, which rearranges to give an "open dimer" complex **10**. This step is (energetically) the most expensive, requiring 11.4 kcal/mol. The complex **10** is a suitable precursor for easy C to N proton transfer via transition state **11**, which lies just 1.2 kcal/mol above **10**. The reaction proceeds via **12**, a second "open dimer" and finally, after extrusion of  $\text{NH}_3$ , yields **14**. The PM3 and ab initio results for the relative energies of these structures are in acceptable agreement; the only exception is the overestimation of the stability of the complex **9** by PM3 (Figure 1). Therefore, PM3 allows comparison of the inter- and intramolecular versions of the deprotonation step with inclusion of solvation, Schemes 3 and 4 and Figure 2, indicating that the intramolecular pathway is preferred by 9 kcal/mol. To assess the reliability of the PM3 method in predicting the geometries of larger complexes in this series, PM3 and MNDO were applied to simulate the X-ray structures of model intermediates such as  $\text{LiC}_6\text{H}_5\text{CHCN} \cdot \text{LDA} \cdot 2 \text{TMEDA}$  (Figure 3),  $[\text{t-BuCN} \cdot \text{LiN}(\text{SiMe}_3)_2]_2$  (Figure 4), and  $[(\text{LiC}_6\text{H}_5\text{CHCN} \cdot \text{TMEDA})_2 \cdot \text{C}_6\text{H}_6]$  (Figure 5). In all cases the LiX subunits are described significantly better by PM3 than by MNDO.

## Introduction

Reaction of nitriles  $\text{RCN}$  ( $\text{R}$  = alkyl, aryl, heteroaryl) with organometallic compounds gives the corresponding addition or deprotonation products.<sup>1</sup> Nitriles with two activated  $\alpha\text{-C-H}$  bonds, such as **1**, react with 2 equiv of base, e.g.,  $\text{LiNR}_2$ , and subsequent alkylation or deuteration to yield disubstituted products **5** (Scheme 1).<sup>2</sup> The following discussion is limited to alkylations, although, in principle, analogous results should be obtained for deuteration.

These experimental findings could lead to the conclusion that a dilithiated intermediate, **6**, plays the central role in this mechanism. However, it has been shown by  $^{13}\text{C}$ -NMR studies that the deprotonations and the alkylations are sequential reactions, i.e., that a dilithio compound of the type **6** is not involved.<sup>3</sup>

The monolithiated structure, which results from the first deprotonation step, aggregates with a second molecule of  $\text{LiNR}_2$  to give a "quasi dianion complex" **2** (QUADAC). These species do not undergo a second deprotonation to yield **6**, but prefer to undergo alkylation

to give an intermediate **3**. The latter must be a relatively stable complex of the nitrile and the lithium amide; otherwise, the nitrile and the "free"  $\text{LiNR}_2$  should compete for the alkylating electrophile. As pointed out by Boche et al., this is not the case, and therefore, the assumption that the second deprotonation step under formation of **4** (which is finally transformed by alkylation to yield **5**) should proceed via an intramolecular pathway seems convincing. This appears to be a remarkable example of the proximity effect as reported for organic and enzymatic reactions.<sup>4</sup>

In solution, both the adduct complex  $\text{R}^1\text{R}^2\text{HCCN} \cdot \text{LiNR}_2$  and the resulting species  $[\text{R}^1\text{R}^2\text{CCN}]^- \cdot \text{Li}^+$  exist as dimers, (**3**)<sub>2</sub> and **4**, respectively. The proposed mechanism is supported by X-ray structures of modified representatives of **2–4**.<sup>5</sup> Unfortunately, interesting and stimulating ab initio calculations,<sup>5b</sup> which were performed for the  $\text{H}_3\text{CCN}/\text{LiNH}_2$  system, do not reflect most of these important details: To simulate a more realistic "ab initio reaction pathway", at least the model base  $\text{LiNH}_2$  should be represented by its dimer,  $[\text{LiNH}_2]_2$ .<sup>6,7</sup>

From the experimental "reality" follows the necessity to include dimeric complexes  $[\text{R}^1\text{R}^2\text{HC-CN} \cdot \text{LiNR}_2]_2$  (**3**) as well as to consider the proposed complexes formed from a dimeric base and the nitrile (substrate) molecule.

\* Abstract published in *Advance ACS Abstracts*, March 1, 1996.

(1) (a) Cram, D. J. *Fundamentals of Carbanion Chemistry*; Academic Press: New York, 1965. (b) Schlosser, M. *Struktur und Reaktivität polarer Organometalle*; Springer: Berlin, 1973. (c) Wakefield, B. J. *Organolithium Compounds*; Pergamon Press: Oxford, 1974. (d) Buncel, E. *Carbanions: Mechanistic and Isotopic Aspects*; Elsevier: Amsterdam, 1975. (e) Stowell, J. C. *Carbanions in Organic Synthesis*; Wiley: New York, 1979. (f) Wilkinson, G.; Stone, F. G. A.; Abel, E. W., Eds. *Comprehensive Organometallic Chemistry*; Pergamon Press: Oxford, 1982, Vol. 1. For theoretical investigations compare: Kaneti, J.; Schleyer, P. v. R.; Clark, T.; Kos, A. J.; Spitznagel, G. W.; Andrade, J.; Moffat, J. B. *J. Am. Chem. Soc.* **1986**, *108*, 1481, and ref 5a.

(2) (a) Kaiser, E. M.; Pretty, J. D.; Knutson, L. A. *Synthesis* **1977**, 509. (b) Zarges, W.; Marsch, M.; Harms, K.; Boche, G. *Angew. Chem.* **1989**, *101*, 1424; *Angew. Chem., Int. Ed. Engl.* **1989**, *28*, 1392.

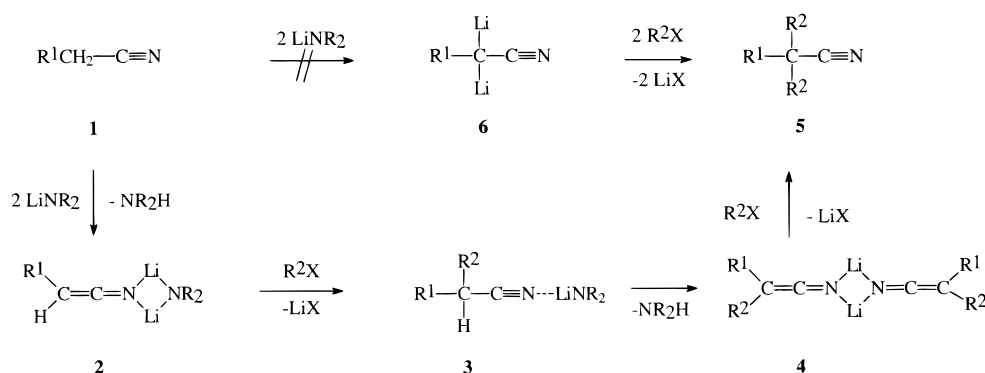
(3) Crowley, P. J.; Leach, M. R.; Meth-Cohn, O.; Wakefield, B. J. *Tetrahedron Lett.* **1986**, *27*, 331.

(4) (a) Bruice, T. C.; Benkovic, S. J. *Bioorganic Mechanism*; Benjamin: New York, 1966; Vol. 1. (b) Houk, K. N.; Tucker, J. A.; Dorigo, A. E. *Acc. Chem. Res.* **1990**, *23*, 107. (c) Menger, F. M. *Acc. Chem. Res.* **1993**, *26*, 206.

(5) (a) **2**: see ref b. (b) Boche, G.; Langlotz, I.; Marsch, M.; Harms, K.; Frenking, G. *Angew. Chem.* **1993**, *105*, 1207; *Angew. Chem., Int. Ed. Engl.* **1993**, *32*, 1171. (c) Boche, G.; Marsch, M.; Harms, K. *Angew. Chem.* **1986**, *98*, 373; *Angew. Chem., Int. Ed. Engl.* **1986**, *25*, 373.

(6) The existence and mechanistic importance of solvated lithium amide dimers,  $[\text{LiNR}_2]_2$ , are well documented. Compare: Collum, D. B. *Acc. Chem. Res.* **1992**, *25*, 448.

(7) Williard, P. G.; Liu, Q.-Y. *J. Am. Chem. Soc.* **1993**, *115*, 3380 and references cited therein.

**Scheme 1. Boche's Deprotonation/Alkylation Cycle for the Formation of C $_{\alpha}$ -Disubstituted Nitriles<sup>5b</sup>**

Consequently, this leads to identical mechanisms for both metalations,  $1 \rightarrow 2$  and  $3 \rightarrow 4$ , respectively. Further, solvent molecules should be included. Ab initio calculations for the resulting "supermolecules" (compare Schemes 3 and 4) would be clearly desirable, but significantly exceed the capacities of most present computers.

In the following we propose a model mechanism based on ab initio and PM3 calculations. We also discuss the competition of *intra*- vs. *intermolecular* deprotonation alternatives, taking account of the role of solvent molecules.

### Method

Ab initio calculations were performed using the Gaussian 92<sup>8</sup> program package. The DFT calculations were carried out with Gaussian 94<sup>9</sup> (Becke3LYP/6-311+G\*) and with DGAUSS<sup>10</sup> (DZP/A1). Semiempirical calculations were run using the program MOPAC6/PC.<sup>11</sup> Geometries were optimized at MNDO,<sup>12</sup> PM3,<sup>13,14</sup> HF/6-31G\*,<sup>15</sup> HF/6-31+G\*,<sup>16</sup> and finally, at MP2(full)/6-31+G\* (i.e., including Møller–Plesset electron correlation<sup>17</sup> in the framework of second order), Becke3LYP/6-311+G\*,<sup>18</sup> and DGAUSS (UniChem) DZP/A1-levels, and characterized as minima, saddle points, etc. by calculation of vibrational frequencies. Our computer capacity does not allow desirable SCF/MP4(sdtq) single point energy calculations of the essential structures 9–14. Zero point energies were scaled

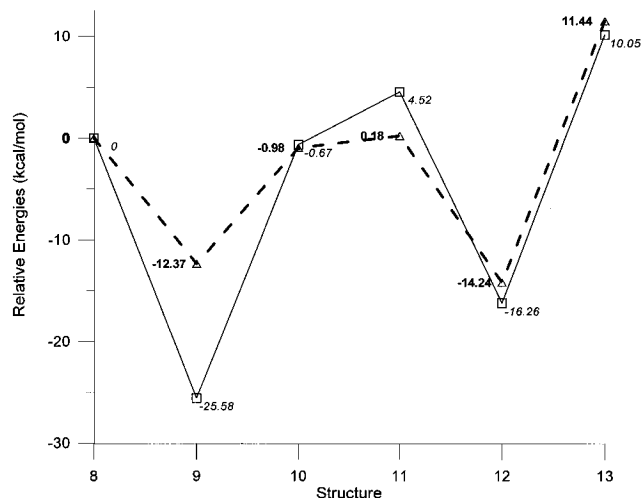


**Figure 1.** Energy Profiles of the *Intramolecular* C $_{\alpha}$ -Deprotonation of MeCN with [LiNH<sub>2</sub>]<sub>2</sub>. Dashed line: MP2(full)6-31+G\*/MP2(full)6-31+G\*. Solid line: PM3 results.

by 0.91.<sup>19</sup> The DFT calculations are part of a cooperation with CRAY Research, Inc.

### Results

**Ab Initio Calculations.** Our model is based on the following considerations: An interesting mechanism for the related deprotonation of  $\alpha$ -CH-activated aldehydes has been proposed previously; it includes several intermediates, whose existence has been confirmed by spectroscopic studies.<sup>7</sup> This mechanism serves, together with the ab initio calculations by Boche et al.,<sup>5b</sup> as an orienting background for the investigations summarized below. Although the limiting factor for high-level ab initio calculations remains the molecular size of the structures 1–14, our model comes closer to reality than the previous theoretical studies, especially as we used [LiNH<sub>2</sub>]<sub>2</sub>, **8**, as the reacting model base complex. Further, we find arguments that solvent molecules must be taken into account. The justification for this statement will be given below. In agreement with Boche's approach, acetonitrile was selected to be the  $\alpha$ -CH-activated model nitrile.

On the basis of our MP2(full)/6-31+G\*/MP2(full)/6-31+G\* calculations (Scheme 2 and Figure 1), the adduct **9**, which is formed from CH<sub>3</sub>CN (**7**) and the dimeric base **8**, is stabilized by about 12 kcal/mol relative to the separated reactants. It is likely that in solution this coordination proceeds by replacement of a solvent mol-

(8) GAUSSIAN 92: Frisch, M. J.; Trucks, G. W.; Head-Gordon, M.; Gill, P. M. W.; Wong, M. W.; Foresman, J. B.; Johnson, B. G.; Schlegel, H. B.; Robb, M. A.; Replogle, E. S.; Gombert, R.; Andres, J. L.; Raghavachari, K.; Binkley, J. S.; Gonzalez, C.; Martin, R. L.; Fox, D. J.; Defrees, D. J.; Baker, J.; Stewart, J. J. P.; Pople, J. A. Gaussian, Inc., Pittsburgh PA, 1992.

(9) GAUSSIAN 94, Revision B.2: Frisch, M. J.; Trucks, G. W.; Schlegel, H. B.; Gill, P. M. W.; Johnson, B. G.; Robb, M. A.; Cheeseman, J. R.; Keith, T.; Petersson, G. A.; Montgomery, J. A.; Raghavachari, K.; Al-Laham, M. A.; Zakrzewski, V. G.; Ortiz, J. V.; Foresman, J. B.; Cioslowski, J.; Stefanov, B. B.; Nanayakkara, A.; Challacombe, M.; Peng, C. Y.; Ayala, P. Y.; Chen, W.; Wong, M. W.; Andres, J. L.; Replogle, E. S.; Gomperts, R.; Martin, R. L.; Fox, D. J.; Binkley, J. S.; Defrees, D. J.; Baker, J.; Stewart, J. J. P.; Head-Gordon, M.; Gonzalez, C.; Pople, J. A. Gaussian, Inc., Pittsburgh PA, 1995.

(10) UniChem 3.01/DGAUSS V3.0. Cray Research, Inc., 1995.

(11) Koch, R.; Wiedel, B. *QCMP* 113; *QCPE Bull.* **1992**, 4, 12. Based on MOPAC 6.0: Stewart, J. J. P. *QCPE* 455, **1990**.

(12) Dewar, M. J. S.; Thiel, W. *J. Am. Chem. Soc.* **1977**, 99, 4899. Li parameters: Thiel, W. *QCPE* 438, *QCPE Bull.* **1982**, 2, 36.

(13) Stewart, J. J. P. *J. Comput. Chem.* **1989**, 10, 209.

(14) Li parameters: Anders, E.; Koch, R.; Freunsch, P. *J. Comput. Chem.* **1993**, 14, 1301.

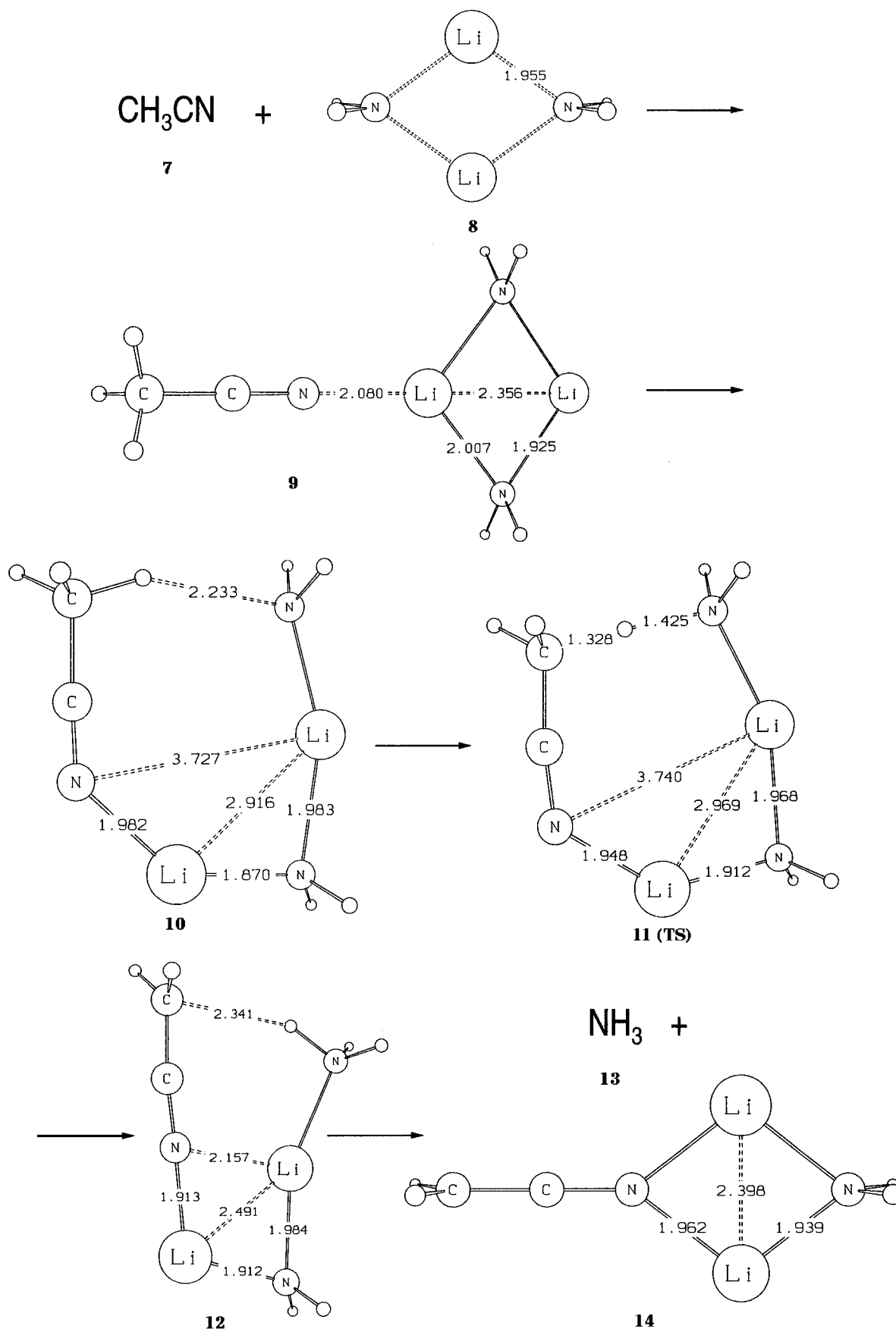
(15) (a) P. C. Hariharan, J. A. Pople, *Theor. Chim. Acta* **1973**, 28, 213. (b) Franci, M. M.; Pietro, W. L.; Hehre, W. L.; Binkley, J. S.; Gordon, M. S.; DeFrees, D. J.; Pople, J. A. *J. Chem. Phys.* **1982**, 77, 3654.

(16) Diffuse functions: Spitznagel, G. W.; Clark, T.; Chandrasekhar, J.; Schleyer, P. v. R. *J. Comput. Chem.* **1982**, 3, 363.

(17) Pople, J. A.; Binkley, J. S.; Seeger, R. *Int. J. Quantum Chem. Symp.* **1976**, 10, 1 and references cited therein.

(18) (a) Becke, A. D. *J. Chem. Phys.* **1986**, 84, 4525. (b) Becke, A. D. *J. Chem. Phys.* **1993**, 98, 5648. (c) Krishnan, R.; Binkley, J. R.; Seeger, R.; Pople, J. A. *J. Chem. Phys.* **1980**, 72, 650.

(19) Grev, R. S.; Jansen, C. L.; Schaefer, H. F., III *J. Chem. Phys.* **1991**, 95, 5128 and references cited therein.

**Scheme 2.** MP2(full)6-31+G\*-Optimized Structures for the Intramolecular C $_{\alpha}$ -Deprotonation of MeCN with [LiNH $_2$ ] $_2$ 

ecule from the dimeric lithium amide. The existence of a complex comparable to **9**<sup>20</sup> and the dimeric character of solvated lithium amides<sup>6,21</sup> are confirmed by NMR

spectroscopy and structural studies. To allow hydrogen transfer from the nitrile to the amide moiety, the central four-membered ring of **9** must open. The resulting

**Table 1.** Energies,<sup>a</sup> Absolute Energies,<sup>b</sup> and Relative Energies<sup>a</sup> of the Structures 7–14

compd	PM3 <sup>a</sup> (NIMAG) <sup>c</sup>	6-31G*// 6-31G* <sup>b</sup>	6-31+G*// 6-31+G* <sup>b</sup>	MP2/6-31+G*// MP2/6-31+G* <sup>b</sup>	ZPE <sup>d</sup> (NIMAG) <sup>e</sup>	Becke3LYP/ 6-311+G*// Becke3LYP/ 6-311+G* <sup>f</sup>	ZPE <sup>f</sup> (NIMAG) <sup>e</sup>	DGauss/ DZVP A1 <sup>g</sup>	ZPE <sup>h</sup> (NIMAG) <sup>e</sup>
<b>7</b>	+23.26	−131.927 534	−131.931 173	−132.345 361	30.62 (0)	−132.791 942	28.46 (0)	−132.728 705	27.70 (0)
<b>8</b>	−23.48	−126.199 408	−126.204 514	−126.578 530	34.79 (0)	−127.099 776	32.82 (0)	−127.007 349	31.85 (0)
<b>9</b>	−25.80	−258.144 446	−258.152 040	−258.942 857	65.93 (0)	−259.907 890	61.75 (0)	−259.752 339	60.72 (0)
<b>10</b>	−0.89	−258.123 038	−258.132 100	−258.925 474	65.40 (0)	−259.893 296	60.98 (0)	not obtained	
<b>11 (TS)</b>	+4.30	−258.111 444	−258.117 865	−258.920 708	63.02 (1)	−259.892 257	59.30 (1)	−259.741 377	58.85 (1)
<b>12</b>	−16.48	−258.142 341	−258.153 342	−258.944 996	66.51 (0)	−259.915 997	62.58 (0)	−259.760 254	60.63 (0)
<b>13</b>	−3.07	−56.184 356	−56.189 499	−56.363 197	23.91 (0)	−56.572 825	21.75 (0)	−56.541 435	21.07 (0)
<b>14</b>	+12.90	−201.923 030	−201.933 143	−202.541 698	40.97 (0)	−203.310 008	38.40 (0)	−203.185 388	37.06 (0)
rel energies					corr <sup>i</sup>		corr <sup>i</sup>		corr <sup>i</sup>
<b>7 + 8</b>	+0.0	+0.0	+0.0	+0.0	+0.0	+0.0	+0.0	+0.0	+0.0
<b>9</b>	−25.58	−10.98	−10.26	−11.90	−12.37	−10.14	−10.57	−10.22	−11.28
<b>10</b>	−0.67	+2.45	+2.25	−0.99	−0.98	−0.99	−0.73		
<b>11</b>	+4.52	+9.73	+11.18	+2.00	+0.18	−0.34	+1.46	−3.34	−2.70
<b>12</b>	−16.26	−9.66	−11.08	−13.24	−14.24	−15.24	−16.42	−15.19	−16.17
<b>13 + 14</b>	+10.05	+12.27	+8.19	+11.92	+11.44	+5.58	+6.60	+5.79	+7.08

<sup>a</sup> Energies in kcal/mol. <sup>b</sup> Absolute energies in atomic units (1 au = 627.51 kcal/mol). <sup>c</sup> Number of **IMAG**inary frequencies. <sup>d</sup> Zero point energies (kcal/mol; 6-31+G\* calculations). <sup>e</sup> Number of **IMAG**inary frequencies (6-31+G\* calculations). <sup>f</sup> Zero point energies (kcal/mol; Becke3LYP/6-311+G\* calculations). <sup>g</sup> UniChem 3.0/optimized using Vosko–Wilk–Nusair (VWN), Becke–Lee–Yang–Paar non-local potential. <sup>h</sup> Zero point energies (kcal/mol; DGauss DZP/A1 calculations). <sup>i</sup> Zero point energy scaled with 0.91.

intermediate **10**, an “open dimer”, is also supported by various investigations of related reaction pathways.<sup>7</sup> The cleavage of an Li–N bond requires about 11 kcal/mol, while the transition state for proton transfer, **11**, lies only just above slightly more than 1 kcal/mol higher in energy than **10**. This low barrier is indicated in a lengthened C–H bond of the open dimer (1.094 Å, compared with 1.082 Å in acetonitrile). After the formation of another “open dimer”, **12**, which is stabilized by 14 kcal/mol relative to the transition state, and extrusion of ammonia, the final intermediate, **14**, is a mixed (dianionic) aggregate of LiNH<sub>2</sub> and LiCH<sub>2</sub>CN, comparable to Boche's QUADAC. The DFT calculations at the Becke3LYP/6-311+G\* level show good agreement with the MP2 results: Stabilization of **9** to **8** results to be about 10 kcal/mol, cleavage of an Li–N bond requires 9 kcal/mol, and the **TS 11** lies about 2 kcal/mol higher in energy than **10**. Unfortunately, it was impossible to localize structure **10** using the DZP/A1 level of theory of DGAUSS.

Further details concerning this deprotonation mechanism, such as the influence of solvation or the possible attack of an external lithium amide, cannot be investigated at this level of ab initio theory due to computer capacity limitations. For this reason, and in order to obtain an additional assessment of our new lithium parameters,<sup>14</sup> we used the semiempirical method PM3 in the following.

**Semiempirical Calculations.** Firstly, we compare the PM3 with the ab initio results. It is a well-known deficiency of semiempirical methods that the stabilities of adduct complexes,<sup>22</sup> such as **9** in Scheme 2, are overestimated, and **9** is indeed found to be much lower in energy with PM3 than at the ab initio levels. With this exception in mind, the ab initio-calculated energy profile for the deprotonation is in good agreement with the PM3 result. Another conclusion from the calculation

of activation energies is the need to use correlated methods (Table 1): at the HF-level (6-31G\* and 6-31+G\* basis sets) the barrier (difference of relative energies between **10** and **11**) is found to be 7.3 and 8.9 kcal/mol, respectively. Taking Møller–Plesset electron correlation into account lowers this barrier to 1.2 kcal/mol. PM3 gives the reasonable result of around 5.2 kcal/mol and thus proves to be well-suited for further investigations in this context. The PM3 bond lengths show acceptable agreement throughout with those obtained by MP2.<sup>23</sup>

As an alternative to the mechanism discussed above, *intermolecular* attack of a base molecule, at least in competition to the *intramolecular* deprotonation, could be plausible. To study this alternative it is necessary explicitly to include solvent molecules, e.g., water as a model for THF. Our calculations reveal that the tendency of Li<sup>+</sup> to saturate its coordination sites would force an additional lithium amide to form an oligomeric cluster with the existing dimer. THF-solvated dimers, as they exist in solution, do not undergo such oligomerizations. We avoided this undesired effect by adding water molecules to the free coordination sites of all lithium atoms. In such a case the incoming lithium amide favors the contact to the CN-moiety.

The appropriate mechanisms for *intra*- and *intermolecular* deprotonation reactions with consideration of solvent molecules are shown in Schemes 3 and 4. Scheme 3 is the analog to the ab initio-calculated *intramolecular* mechanism, now including solvation, and needs no further discussion. Scheme 4 represents the *intermolecular* deprotonation pathway. The external base [LiNH<sub>2</sub>]<sub>2</sub>·4S (**15**, S = H<sub>2</sub>O) attacks the adduct **16** to give **17**, in which the incoming dimeric amide coordinates with the CN-triple bond. The 4-ring then opens to give an open dimer (lower part of **18a**, which is the analog of **18**); this ring opening affords about 18.6 kcal/mol. In **18a**, one proton already faces the NH<sub>2</sub> anion. Again,

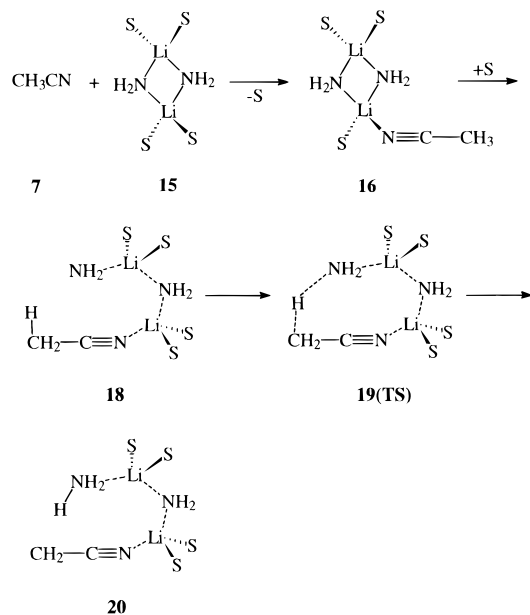
(20) Compare the X-ray data of [*t*-Bu-Li(NSiMe<sub>3</sub>)<sub>2</sub>]<sub>2</sub> published by Boche, G. et al.<sup>5b</sup>

(21) (a) Gilchrist, J. H.; Collum, D. B. *J. Am. Chem. Soc.* **1992**, *114*, 794. (b) Romesberg, F. E.; Collum, D. B. *J. Am. Chem. Soc.* **1992**, *114*, 2112. (c) Bernstein, M. P.; Romesberg, F. E.; Fuller, D. J.; Harrison, A. T.; Collum, D. B.; Liu, Q.-Y.; Williard, P. G. *J. Am. Chem. Soc.* **1992**, *114*, 5100.

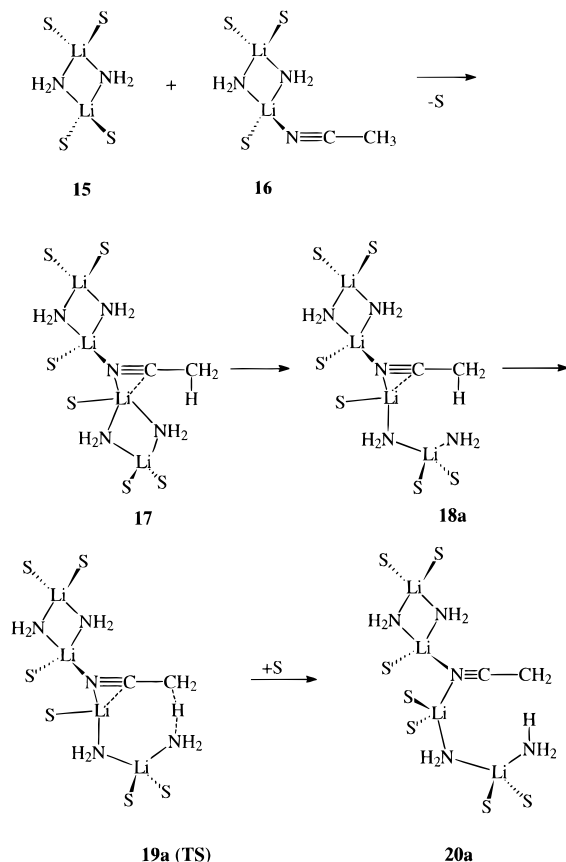
(22) Opitz, A.; Koch, R.; Katritzky, A. R.; Fan, W. Q.; Anders, E. *J. Org. Chem.* **1995**, *60*, 3743.

(23) The transition state **11** (Scheme 2) may serve as a representative (MP2(full)/6-31+G\*; values in brackets: PM3 results). Bond length (Å): C–C, 1.421 (1.404); C–H, 1.328 (1.382); N(3)–H, 1.425 (1.405); C–N(1), 1.190 (1.182); Li(1)–N(1), 1.948 (1.959); Li(1)–N(2), 1.912 (1.943); Li(2)–N(2), 1.968 (1.976). Deviations between HF/6-31+G\* and MP2(full)/6-31+G\* are found for the N(3)–H (HF: 1.385, MP2: 1.425 Å) and the C–H bond (HF: 1.359, MP2: 1.382 Å).

**Scheme 3. Intermediates and the Transition State in the Course of the Intramolecular Deprotonation of MeCN with Solvated Dimeric  $[\text{LiNH}_2]_2$  ( $\text{S} = \text{H}_2\text{O}$ )**



**Scheme 4. Intermediates and the Transition State in the Course of the Intermolecular Deprotonation of MeCN with Solvated Dimeric  $[\text{LiNH}_2]_2$  ( $\text{S} = \text{H}_2\text{O}$ )**



proton transfer (C to N) is energetically facile (1.3 kcal/mol, formation of TS **19a**). Finally, the product **20a** is formed, thereby releasing 22 kcal/mol. The energy profiles (Figure 2) reveal a strong preference for the intramolecular reaction by about 9 kcal/mol. This result confirms the validity of the *ab initio*-based mechanism,

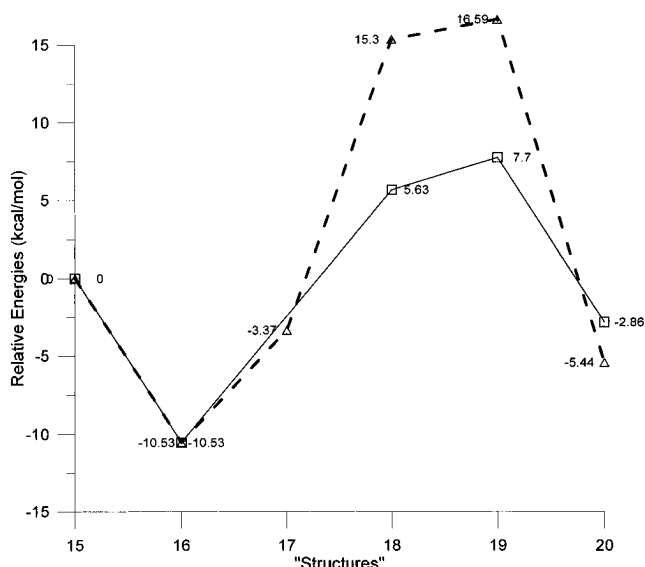


**Figure 2.** Energy profiles which correspond to Schemes 3 and 4: For intramolecular mechanism, compare Scheme 3,  $\text{S} = \text{H}_2\text{O}$ . Solid line: I  $\equiv$  **7** + **15**; II  $\equiv$  **16** +  $\text{S}$ ; IV  $\equiv$  **18**; V  $\equiv$  **19** (TS); VI  $\equiv$  **20**. For intermolecular mechanism, compare Scheme 4. Dashed line: I  $\equiv$  **7** + 2 **15**; II  $\equiv$  **15** + **16** +  $\text{S}$ ; III  $\equiv$  **17** + 2  $\text{S}$ ; IV  $\equiv$  **18a** + 2 $\text{S}$ ; V  $\equiv$  **19a** (TS) + 2 $\text{S}$ ; VI  $\equiv$  **20a** +  $\text{S}$ . Absolute energies: see Table 5.

which had neglected the possibility of external attack and, furthermore, supports the reaction sequence postulated by Boche (Scheme 1), in which intermediate **3** transforms into **4** by intramolecular reaction due to a significant proximity effect. Although an uncertainty remains resulting from the PM3 tendency to overestimate the stabilities of the initially formed complexes (the "solvated" type **16**, Figure 2, and its "unsolvated" counterpart **9**, Figure 1), the energy for the Li–N bond cleavage under formation of open dimers and the activation barrier of the C to N proton transfer appear to decrease under the influence of solvent molecules.

**Comparison with X-ray Structures.** As mentioned above, the proposed intermediates are strongly supported by three X-ray structures. In the final part of this paper, we calculated these species using both PM3 and MNDO and compared the results with the experimentally determined data. Both semiempirical methods reveal the important structural features. Therefore, only a description of the structure itself and the relevant lithium bonds is given for each molecule.

The assumption of a QUADAC as the first intermediate **2** in the lithiation of nitriles (Scheme 1) was supported by the solid state structure of  $\alpha$ -lithiophenylacetonitrile·lithiumdiisopropylamide·2 TMEDA (Figure 3, Table 2).<sup>5a</sup> Lithium and nitrogen atoms form the central four-membered ring segment. PM3 is distinctly superior to MNDO in the representation of all the lithium bonds, especially for the Li–TMEDA contacts.

The second X-ray structure corresponds to model compound **3** in Scheme 1.<sup>5b</sup> It is a dimeric *tert*-butylcyanide·lithiumbis(trimethylsilyl)amide with the lithium and nitrogen atoms of the base forming a four-membered ring and the nitrile coordinating to the lithium atoms (Figure 4, Table 3). The first point to note is the lengthening of the N–Si bonds, possibly due to deficiencies in the parametrization of silicon. In good agreement with the experimental structure, PM3 finds a steplike arrangement of the cyano groups relative to the ring. In

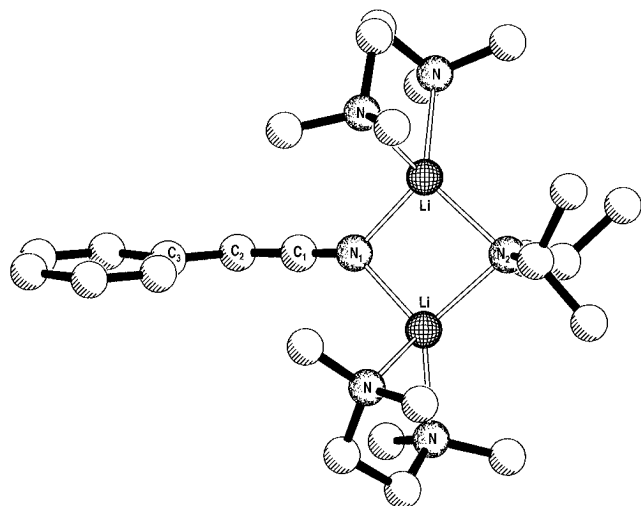


**Figure 3.** PM3-calculated structure of  $\text{LiC}_6\text{H}_5\text{CHCN}\cdot\text{LDA}\cdot 2\text{TMEDA}$ .

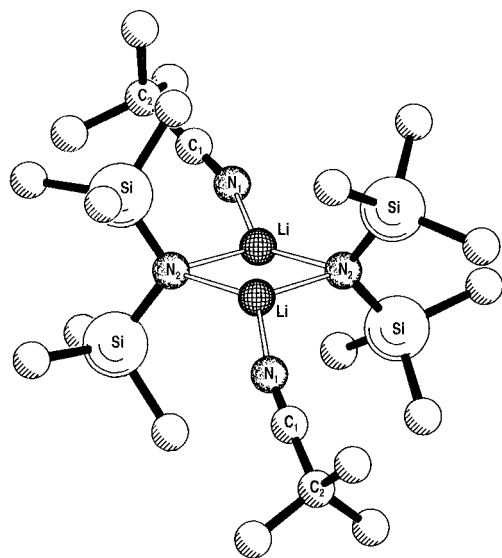


**Figure 4.** PM3-calculated structure of  $[t\text{-BuCN}\cdot\text{LiN}(\text{SiMe}_3)_2]_2$ .

**Table 2. Selected Structural Parameters of  $\text{LiC}_6\text{H}_5\text{CHCN}\cdot\text{LDA}\cdot 2\text{TMEDA}$**

	X-ray	PM3	MNDO
bond lengths (Å)			
Li–N <sub>1</sub>	2.092(9)	2.059	2.225
Li–N <sub>2</sub>	2.035(8)	2.127	2.236
Li–N <sub>TMEDA</sub>	2.268(9)	2.240	2.523
N <sub>1</sub> –C <sub>1</sub>	1.173(7)	1.209	1.193
C <sub>1</sub> –C <sub>2</sub>	1.383(8)	1.347	1.365
C <sub>2</sub> –C <sub>3</sub>	1.432(8)	1.434	1.437
bond angles (deg)			
C <sub>2</sub> –C <sub>1</sub> –N <sub>1</sub>	179.5(7)	179.7	177.9
N <sub>1</sub> –Li–N <sub>2</sub>	98.7(4)	93.4	92.8
Li–N <sub>2</sub> –Li	82.7(3)	84.0	85.8
Li–N <sub>1</sub> –Li	80.0(3)	87.5	86.3
N <sub>1</sub> –Li–N <sub>TMEDA</sub>	104.7(3)	111.1	111.4
N <sub>2</sub> –Li–N <sub>TMEDA</sub>	132.0(4)	129.0	133.2

contrast, MNDO predicts a linear coordination (bond angle C<sub>1</sub>–N<sub>1</sub>–Li). PM3 is again the preferred method for this structure with more exact bond lengths and angles.

The crystal structure of  $[(\alpha\text{-cyanobenzyl}^-\text{lithium}^+\cdot\text{TMEDA})_2\cdot\text{C}_6\text{H}_6]$ , which is a representative of intermediate 4, (Figure 5, Table 4), serves as the missing link.<sup>5c</sup> The dimeric unit crystallizes with one benzene molecule,

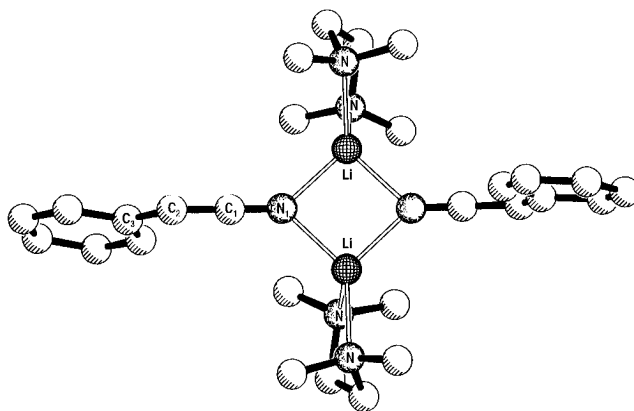


**Figure 5.** PM3-calculated structure of  $[(\text{LiC}_6\text{H}_5\text{CHCN}\cdot\text{TMEDA})_2\cdot\text{C}_6\text{H}_6]$ ; benzene is not included in the calculations.

**Table 3. Selected Structural Parameters of  $[t\text{-BuCN}\cdot\text{LiN}(\text{SiMe}_3)_2]_2$**

	X-ray	PM3	MNDO
bond lengths (Å)			
Li–N <sub>1</sub>	2.049(8)	1.987	2.232
Li–N <sub>2</sub>	2.030(7)	2.040	2.171
N <sub>2</sub> –Si	1.700(3)	1.782	1.712
N <sub>1</sub> –C <sub>1</sub>	1.139(6)	1.161	1.161
C <sub>1</sub> –C <sub>2</sub>	1.461(7)	1.468	1.474
bond angles (deg)			
N <sub>1</sub> –C <sub>1</sub> –C <sub>2</sub>	179.6(4)	177.8	179.9
N <sub>2</sub> –Li–N <sub>2a</sub>	105.1(3)	103.7	110.5
Li–N <sub>2</sub> –Li	74.9(3)	76.3	69.5
C <sub>1</sub> –N <sub>1</sub> –Li	161.5(4)	158.3	179.1
N <sub>1</sub> –Li–N <sub>2</sub>	115.9(3)	115.0	123.6
	139.0(4)	135.9	125.8

**Table 4. Selected Structural Parameters of  $[(\text{LiC}_6\text{H}_5\text{CHCN}\cdot\text{TMEDA})_2\cdot\text{C}_6\text{H}_6]$**

	X-ray	PM3	MNDO
bond lengths (Å)			
Li–N <sub>1</sub>	2.04(3)	2.035	2.167
Li–N <sub>TMEDA</sub>	2.05(4)	2.181	2.312
Li–Li	2.64(5)	2.731	3.011
N <sub>1</sub> –C <sub>1</sub>	1.17(7)	1.212	1.196
C <sub>1</sub> –C <sub>2</sub>	1.38(2)	1.342	1.360
C <sub>2</sub> –C <sub>3</sub>	1.43(2)	1.437	1.442
bond angles (deg)			
C <sub>3</sub> –C <sub>2</sub> –C <sub>1</sub>	124.5(1)	123.9	127.3
C <sub>2</sub> –C <sub>1</sub> –N <sub>1</sub>	178.4(1)	178.4	177.3
N <sub>1</sub> –Li–N <sub>1a</sub>	98.2(0.5)	93.3	92.0
Li–N <sub>1</sub> –Li	80.9(0.5)	84.3	88.0

**Table 5. Absolute Energies (kcal/mol) of PM3-Calculated Structures; See Figure 2**

	CH <sub>3</sub> CN	H <sub>2</sub> O	
<b>15</b>	–281.39	<b>16</b>	–215.23
		<b>17</b>	–436.03
<b>18</b>	–252.50	<b>18a</b>	–417.36
<b>19 (TS)</b>	–250.43	<b>19a (TS)</b>	–416.07
<b>20</b>	–260.99	<b>20a</b>	–496.94

which was neglected in the calculations because the shortest distance of benzene to the lithiated species is about 4 Å. The lithium and nitrogen centers once more form a four-membered central ring with two molecules of TMEDA as the solvent. PM3 is again superior over MNDO in the reproduction of most of the geometrical parameters.

## Conclusion

The interplay between experimental, ab initio, and semiempirical methods led us to conclude that the

deprotonation of  $\alpha$ -CH-activated nitriles with dimeric lithium amides prefers the *intramolecular* route. The *intermolecular* pathway is significantly disfavored. PM3 reproduces the experimentally determined geometries of the model structures to an acceptable extent and, therefore, again proves to be a useful tool to investigate lithiated structures, and their reaction modes.<sup>14,22,24–32</sup>

**Acknowledgment.** The authors are pleased to acknowledge research support by the Fonds der

Chemischen Industrie (Germany) and the Deutsche Forschungsgemeinschaft. They thank Prof. Dr. G. Boche (Marburg) for useful discussions. They also want to thank Cray Research, Inc. for the UniChem program package and a significant amount of supercomputer CPU-time.

JO9519470

(24) Katritzky, A. R.; Ignatchenko, A. V.; Lan, X.; Lang, H.; Opitz, A.; Koch, R.; Anders, E. *Tetrahedron* **1994**, *50*, 6005.

(25) Koch, R.; Anders, E. *J. Org. Chem.* **1994**, *59*, 4529.

(26) Koch, R.; Anders, E. *J. Org. Chem.* **1995**, *60*, 5861.

(27) Wenzel, M.; Lindauer, D.; Beckert, R.; Boese, R.; Anders, E. *Chem. Ber.* **1996**, *129*, 39.

(28) Gertzmann, R.; Möller, M. H.; Rodewald, U.; Fröhlich, R.; Grehl, M.; Würthwein, E. U. *Tetrahedron* **1995**, *51*, 3767.

(29) Gertzmann, R.; Fröhlich, R.; Grehl, M.; Würthwein, E. U. *Tetrahedron* **1995**, *51*, 9031.

(30) Kōnemann, M.; Erker, G.; Grehl, M.; Fröhlich, R.; Würthwein, E. U. *J. Am. Chem. Soc.* **1996**, in press.

(31) Pratt, L. M.; Khan, I. M. *J. Comput. Chem.* **1995**, *9*, 1067.

(32) Haller J.; Hense T.; Hoppe D. *Liebigs Ann. Chem.* **1996**, in press.